Hindawi Publishing Corporation
International Journal of Antennas and Propagation
Volume 2013, Article ID 305362, 6 pages
http://dx.doi.org/10.1155/2013/305362

Research Article

Electric Field Measurement of the Living Human Body for Biomedical Applications: Phase Measurement of the Electric Field Intensity

Ichiro Hieda[1] and Ki Chang Nam[2]

[1] *National Institute of Advanced Industrial Science and Technology (AIST), Tsukuba 305-8566, Japan*
[2] *Yonsei University College of Medicine, Seoul 120-752, Republic of Korea*

Correspondence should be addressed to Ichiro Hieda; i-hieda@aist.go.jp

Received 20 June 2013; Revised 30 August 2013; Accepted 8 October 2013

Academic Editor: Yifan Chen

The authors are developing a technique for conducting measurements inside the human body by applying a weak electric field at a radio frequency (RF). Low RF power is fed to a small antenna, and a similar antenna located 15–50 cm away measures the electric field intensity. Although the resolution of the method is low, it is simple, safe, cost-effective, and able to be used for biomedical applications. One of the technical issues suggested by the authors' previous studies was that the signal pattern acquired from measurement of a human body was essentially different from that acquired from a phantom. To trace the causes of this difference, the accuracy of the phase measurements was improved. This paper describes the new experimental system that can measure the signal phase and amplitude and reports the results of experiments measuring a human body and a phantom. The results were analyzed and then discussed in terms of their contribution to the phase measurement.

1. Introduction

The authors are developing a technique for conducting measurements inside the human body by applying a weak electric field at radio frequency (RF), typically 1–60 MHz [1, 2].

Technological advancements have led to the development of high-level diagnostic techniques, including X-ray computed tomography (X-ray CT), magnetic resonance imaging (MRI), and positron emission tomography (PET), which have contributed greatly to medical care and welfare. However, such high-level care and large-scale medical equipment represent financial burdens to taxpayers in most developed countries. Moreover, due to these costs, people in developing countries rarely benefit from these high-level diagnostic techniques. From this perspective, simple and easy-to-use equipment utilizing electric impedance and magnetic induction is expected [3–6]. The authors started to apply the radio imaging method, which was originally used for geological survey (RIM), to the measurement of the human body [2, 7, 8]. Later, the evolved technique was classified as an electric field method [9, 10].

There are several studies of biomedical measurements that use an electromagnetic wave. One example is microwave tomography. The basic principle of their projects is similar to our proposal. To obtain finer resolution less than 1 cm, pulse signals and multiple antennas for transmitting and receiving were implemented [11–14]. Because attenuation in the human body at the microwave frequency range is remarkable, an electromagnetic darkroom is necessary to prevent interference of an electromagnetic wave along indirect paths as well as to suppress emission of the microwave to the outside environment.

The authors' method is simple, safe, and cost-effective and leads to the expectation of two goals. One is the extension of the current experimental system, which can be applied to medical screenings such as abdominal fat CT.

Another goal is smaller systems able to be used as wearable sensors or installed at home, such as urine volume sensors and dehydration alarms, for welfare and health care.

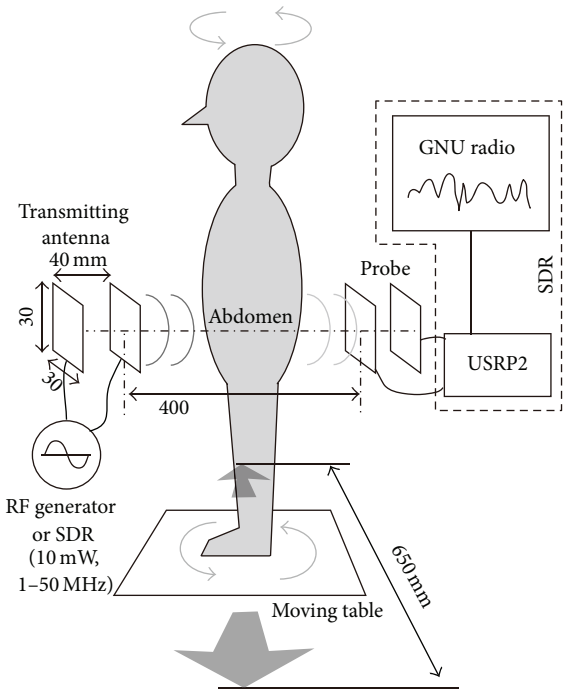

Figure 1: Overview of the experiment. A subject stood still on the moving table. The transmitting antenna and the probe were set at the height of the abdomen of the subject. USRP comprised an RF front end and A/D converter that worked as a software-defined radio (SDR) in conjunction with GNU Radio software installed on a PC.

Figure 1 shows an overview of the developed system. A portion of the human body was scanned by a weak electric field at radio frequency (RF), and the measured signals were analyzed to obtain the permittivity that corresponded to the moisture distribution inside the body.

Experiments were performed in previous studies to determine basic characteristics of the method. To support the experimental results, the measurement system was numerically simulated using the finite-difference time-domain (FDTD) method [15–19]. One of the technical issues suggested by these previous studies was that when the human body was measured, the pattern of the electric field intensity differed from that of a phantom [1, 17].

When the system scanned the phantom, an acrylic water tank filled with water, the electric field intensity at the receiving antenna increased due to the high relative permittivity of the water, which was approximately 70. In contrast, human body tissues have a variety of permittivities. The permittivities of tissues containing much moisture, for example, muscles and internal organs, are as high as those of water at room temperature and pressure [20]. Therefore, water was used for the medium of the phantom to simulate a portion of the human body that contains much moisture.

When the system scanned the living human body, however, the electric field intensity decreased. This was caused by RF current leakage through the human body, which had much larger dimensions and a much tighter electrostatic connection to the electric ground than the phantom. It was experimentally confirmed that measurement of signal strength was simple subtraction of the loss from the increment caused by current leakage and permittivity, respectively [17]. Because the signal attenuation from the current leakage was dominant, the effect of the human body permittivity was buried in the measurement data. Improving the phase measurement capability of the electric field intensity would help to discriminate the effect of permittivity from signal attenuation caused by the current leakage.

In this paper, a new experimental system that can measure the signal phase and amplitude is described. Experiments are also reported where the human body and a phantom were measured by the system. The results were analyzed and discussed in terms of their contribution to the phase measurement.

2. Method

2.1. Experimental System. Figure 2 shows a schematic block diagram of the experimental system. The system comprised transmitting (TX) and receiving (RX) subsystems. Both of the subsystems had a software-defined radio (SDR), an amplifier, an RF transformer, and an antenna.

An SDR is a radio communication system with minimal hardware, and most of the functions are implemented by means of computer software [21, 22]. The experimental system had two hardware peripherals, Ettus Research USRP N200 and USRP2, for transmitting and receiving, respectively [23]. Each peripheral had a high-speed analog-to-digital converter (ADC) and a digital-to-analog converter (DAC). They sent and received digital streaming data to and from personal computers (PCs) via gigabit Ethernet interfaces. GNU Radio, an open source SDR software, was installed on the PCs and was optimized for the USRP series of SDR peripherals [24].

The RX subsystem was the same as that of the previous experimental system [22], except that the reference clock was fed by the external base frequency oscillator instead of the internal clock. The receiving antenna generated a signal in accordance with the electric field intensity, and this signal was fed to USRP2 via both an RF transformer and an amplifier. The received signal was filtered and stored on the computer (PC1) by the SDR software. The USRP N200 series was the successor of the USRP2 series, and both series have the same basic performance and functions. PC1 and PC2 were desktop computers with Intel Core i7 processors.

The previous TX subsystem comprised a battery-powered oscillator and an antenna to simplify the system [25]. The new system added another SDR (SDR2) to the TX subsystem, as shown in Figure 2. A continuous wave (CW) at a certain frequency can be generated by SDR2. In the experiment described in this paper, only a 48 MHz CW was used. The output of the SDR was amplified by the external amplifier and approximately 10 mW of the RF power was fed to the TX antenna. The reference clock of the USRP2 was provided by the same base frequency oscillator as the RX subsystem.

Because the two SDR peripherals (USRP2 and USRP N200) had the same reference clock, their internal oscillators were locked in phase. If the transmitting and receiving

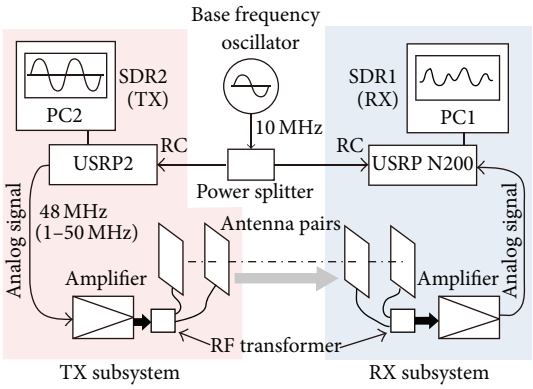

Figure 2: Schematic block diagram of the experimental system. The system consisted of TX and RX subsystems and a base frequency oscillator. Both of the subsystems had a PC, a USRP (SDR peripheral), an external amplifier, an RF transformer, and an antenna. Because the two USRPs had the same reference clock, the internal oscillators were locked in phase.

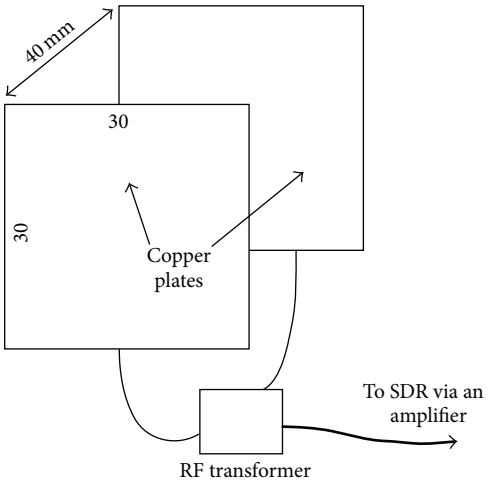

Figure 3: Illustration of an antenna. Two square copper plates were set 40 mm apart. The same types of antennas were used for transmitting and receiving.

frequencies were set to the same frequency, the RX SDR could measure not only the amplitude of the signal transmitted by the TX SDR but also the phase of the signal. This was a great advantage of the new system compared to the previous system.

Figure 3 shows the antennas used in the experiment. They were made of thin copper plates measuring 30 mm^2. The two plates were set parallel 40 mm apart. Antennas of the same type were set 400 mm apart and used for both transmitting and receiving. Because the antennas and RF transformers were optimized to generate and detect electric fields, the emission of electromagnetic waves from the TX antenna was very weak. The reinforced concrete walls and ceilings of the building were able to prevent emission to the outside.

2.1.1. Experiment 1. Figure 4 shows the configuration of the water tank measurement. An acrylic water tank filled with

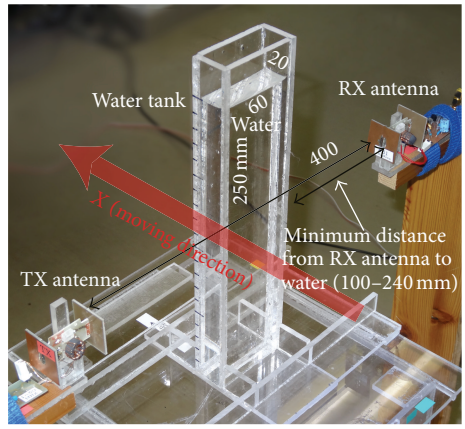

Figure 4: Overview of the water measurement. The water tank moved in between the TX and RX antennas so that the water was scanned by the antenna system one dimensionally. The minimum distance from the RX antenna to the inside of the water tank could be configured from 100 to 240 mm.

water was used as the phantom to simulate a portion of the human body. The inside dimensions of the water tank were 20(W) × 60(D) × 250(H) mm, and the tank was filled with water at room temperature. The relative permittivity of water at room temperature and pressure is approximately 70, which is as high as some human organs, such as muscles and internal organs [20]. The relative permittivity of the acrylic was approximately 4, and the walls of the tank were 5 mm thick. The effect of the walls on the electric field was negligible.

The dimensions of the water tank were much smaller than the actual human body. It was confirmed by experiments and simulation in our previous studies that addition and subtraction of dielectric material in the measured space worked [2, 26]. By changing the position of the water tank, the changes of the electric field intensity were measured. The summation of certain regions of the measurement was equivalent to the result of a large phantom that was as large as the measured region of the small phantom. Moreover, the small tank was convenient to evaluate the effect of a certain region on the measurement result or sensitivity.

The water tank was put on a motor-driven acrylic table. The water tank moved 650 mm in a straight line perpendicular to the centerline of the transmitting and receiving antennas. Signal strength was measured continuously while the water tank moved. The measurement was repeated 10 times for each line.

2.1.2. Experiment 2. Figure 1 shows an overview of Experiment 2. The abdomen of a healthy male subject, 54 years old, 168 cm tall, and weighing 61.5 kg, was measured. The moving table moved straight 650 mm to scan the abdomen of the subject with the antenna pair one dimensionally. The subject stood still on the table facing perpendicular to the moving direction so that the one-dimensional back projection of the abdomen was measured. Both forward and backward measurements were performed. The measurement took approximately two minutes. The authors are planning

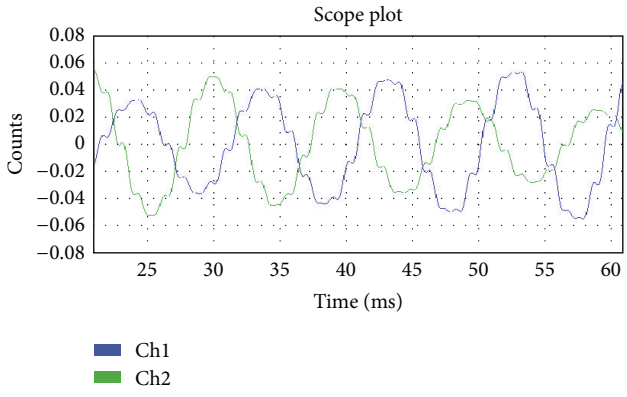

(a) TX and RX are not synchronized

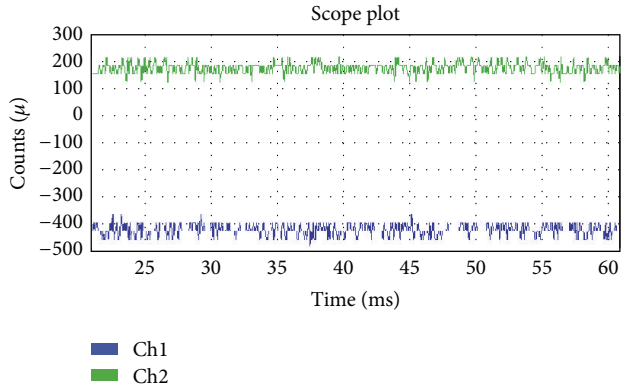

(b) TX and RX are synchronized

FIGURE 5: I/Q outputs from the SDR peripheral. The blue and green lines show the I and Q signals, respectively.

to measure a subject from 16 directions to build a two-dimensional image. The measurement takes approximately 30 minutes. It was confirmed by preliminary experiment that 30 minutes was the limit for a normal adult to stand on the moving table calmly. This is the reason that the subject was only measured twice in two minutes.

3. Results and Discussion

Figure 5 shows SDR outputs for a period of 40 ms where (a) TX and RX SDRs used independent internal reference clocks and (b) TX and RX SDR used the same reference clock, respectively. The RX SDR provides I/Q data that had phase information of the time domain signal as well as magnitude [21]. The I/Q data were stored and processed by the computers in the form of a complex number.

Figure 5(a) shows the received signals where the TX and RX SDRs were connected to each other by a coaxial cable. Both of the I/Q signals were sinusoidal waves with a small level of harmonics. From the figure, the base frequency of the waves was calculated as 103 Hz or 2.14 ppm of the fundamental frequency, 48 MHz.

In Figure 5(b), a portion of the received signal in Experiment 1 is shown. The I/Q signals were DC with a small level of random noise. Because the fundamental frequency of the signals was 0 Hz, the TX and RX SDRs were confirmed to be

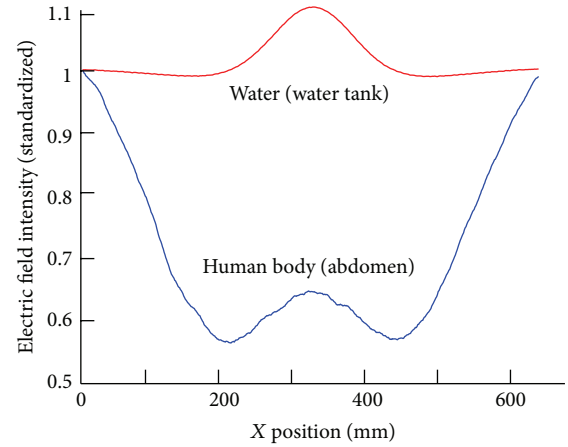

FIGURE 6: Relation between (Y) electric field intensity and (X) distance of the water tank and the living human body from the home position where the data were averaged for the 10 and 2 measurements, respectively. Both of the electric field intensities were standardized by the respective values as the starting point or $X = 0$.

synchronized. When the SDRs were synchronized, the phase difference between TX and RX, θ, was calculated by

$$\theta = \tan^{-1}\frac{Q}{I}, \tag{1}$$

where I and Q were signed amplitudes of the I and Q signals, respectively.

Figure 6 shows the relationships between electric field intensities and phases versus the position of the water tank and the living human body. Each electric field intensity was standardized by the respective value of the starting point, or $X = 0$. The electric field intensities of the water tank and abdomen were averages of 10 and 2 measurements, respectively. The patterns of the signal changes matched the results of previous experiments [1, 22].

As shown in Figure 6, when the water was measured, the electric field intensity increased gradually and made a broad peak. After the peak, the electric field intensity decreased symmetrically. The width of the water in the tank was only 20 mm; however, the skirt of the measured data was as wide as 200 mm. Because the signal changes caused by permittivity of water were steady and reproducible, the data could be used to build reverse filters for the measured data [27–30].

As shown in the same figure, the pattern of the electric field intensity for the living human body was more complex than that of the phantom. The electric field intensity drastically decreased to 55% of the strength at the starting point and then increased to a small peak, as high as 65%. After the electric field intensity decreased to a second trough, it increased up to the starting level. The signal changes were nearly symmetrical. The abdomen of the subject was as wide as 330 mm; however, the electric field intensity was affected by the living body for 650 mm, the total length of the table movement. In the case of the living body measurement, the attenuation of the electric field intensity, which was caused by current flowing to the virtual ground through the human

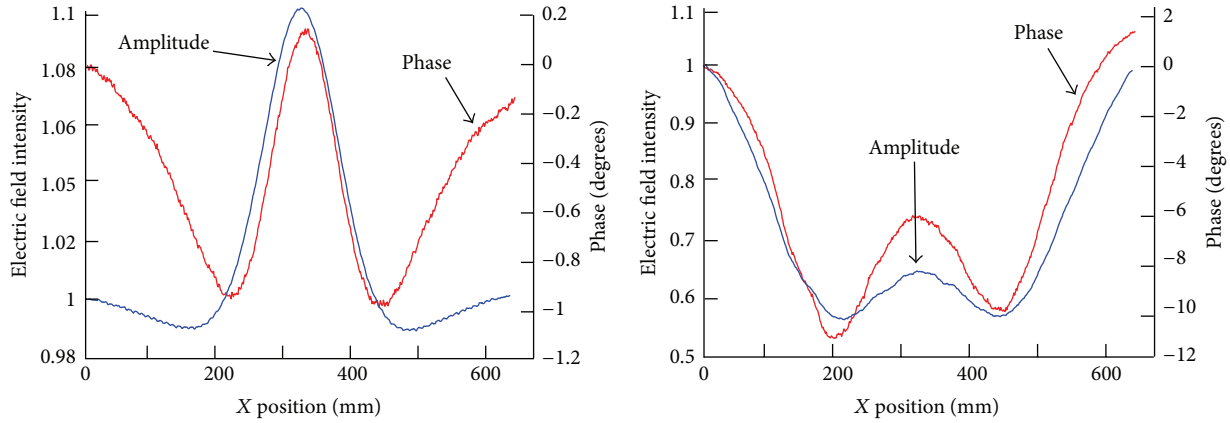

(a) Water inside the water tank

(b) Abdomen of the living human body

FIGURE 7: Amplitude and phase of the electric field intensity against X position.

body and had larger dimensions and static induction to the ground than the water tank, was dominant [17].

The purpose of the study was to obtain a clue to extract the permittivity-induced signal increase from the attenuation caused by the body current. Consequently, the experimental system was upgraded.

Figures 7(a) and 7(b) show the phase changes of the measured signals that were calculated from the I/Q data of the water tank and the human abdomen measurements, respectively, along with the electric field intensities redrawn from the data in Figure 6. Although the phases were provided, the absolute phase reference of the signals was unable to be obtained by the current system. Therefore, the signal received when the moving table was at the starting point, $X = 0$, was defined as the reference for the measurement. Phases in the figures represent differences between the respective reference phases.

In Figure 7(a), the phase decreased from the starting point and reached −1 degree, where $X = 220$ mm. At that point, the phase increased sharply along with the electric field intensity and recovered to the original value at the center of the moving table path. However, the peak positions of the electric field intensity and the phase were 6 mm apart. After the peaks, both of the values decreased to their previous minimum values. The phase recovered again and returned approximately to the original value.

The phase axis in the figure was magnified to understand the characteristics easily; however, the range of the phase was from zero to −1 degree at most. The electric field intensity increased 10% at the peak.

The measurement was done in the near field of the transmission and receiving antennas. The dielectric material, such as water or the human body, caused irregularity of the electric field. As a result, the electric field intensity at the receiving antenna increased or decreased. The authors also confirmed this effect by FDTD simulation [15].

When the human body was measured by the method, the electric field intensity at the receiving antenna was weakened by the effect of leakage current that flowed to the ground of the environment. This effect was observed in a simplified experiment [17]. The connection between the human body and the ground of the environment has not been modeled, so the behavior of the current has not been simulated.

The phase changes of the electric field in Figures 7(a) and 7(b) were not significant compared with the changes of the electric field intensity. Moreover, the phase and the respective intensity were interdependent. The phase itself did not work to abstract the effects of the permittivity from the loss caused by the body current.

The experimental system was upgraded and the phase measurement function was verified by the experiment. Notably, the phase patterns of the electric field intensity and the phase of the living body were different from those of the phantom as well as the amplitude of the electric field intensity.

However, it was difficult to discriminate losses caused by the body current from the increase in the electric field intensity by the permittivity of the moisture using the provided data themselves. The phase was important but not sufficient to discriminate them.

Using multiple frequencies may help to discriminate the permittivity's effects from the current losses. The upgraded system can measure amplitude and phase from 1 to 60 MHz, but optimum antenna systems for the measurement frequencies should be built and tuned for each measurement frequency [17].

The phase started changing at the first measurement point. Therefore, it may also be necessary to extend the travel path of the moving table by upgrading the measurement system. Simulation of a total experimental room including the subject body by a large-scale commercial FDTD simulator package should be effective for the investigation of the body current as well.

4. Conclusion

A new experimental system was introduced that could measure the phase and amplitude of the electric field intensity. Using the system, basic measurements were performed using a water tank and a living human body. The phases at a radio frequency, 48 MHz, were confirmed by measurement results

to be properly measured. Because an SDR with software developed by an open source project was used, the system is simple and cost-effective.

The phase of the measured signal was important information to discriminate the signal increase by the permittivity of moisture from the signal decrease by the current losses. However, the phases and the amplitudes were interdependent. Therefore, the development of an additional method, for example, the use of multiple antennas and a wide range of frequencies, is necessary.

References

[1] I. Hieda and K. C. Nam, "Electric field measurement for biomedical application—characteristics of raw measurement data," in *Proceedings of the International Conference on Biomedical Engineering and Biotechnology*, pp. 789–792, IEEE Computer Society, 2012.

[2] I. Hieda and K. C. Nam, "2D image construction from low resolution response of a new non-invasive measurement for medical application," *ETRI Journal*, vol. 27, no. 4, pp. 385–393, 2005.

[3] J. G. Webster, Ed., *Electrical Impedance Tomography*, Adam Hilger, New York, NY, USA, 1990.

[4] S. Grimnes and O. G. Martinsen, *Bioimpedance and Bioelectricity Basics*, Academic Press, London, UK, 2000.

[5] H. Scharfetter, H. K. Lackner, and J. Rosell, "Magnetic induction tomography: hardware for multi-frequency measurements in biological tissues," *Physiological Measurement*, vol. 22, no. 1, pp. 131–146, 2001.

[6] A. Korjenevsky, V. Cherepenin, and S. Sapetsky, "Magnetic induction tomography: experimental realization," *Physiological Measurement*, vol. 21, no. 1, pp. 89–94, 2000.

[7] G. Rogers, L. Brandt, J. Young, and J. Kot, "The Study of diffusion effect in RIM tomographic imaging," *Exploration Geophysics*, vol. 24, pp. 785–788, 1993.

[8] J. Young, G. Rogers, S. Thomson, and M. Neil, "Australian development of tomographic radio imaging as a new tool in mining geophysics," *Butsuri-Tansa*, vol. 47, pp. 249–255, 1994.

[9] T. S. Tuykin and A. V. Korjenevsky, "Electric field tomography system with planar electrode array," in *Proceedings of the 13th International Conference on Electrical Bioimpedance and the 8th Conference on Electrical Impedance Tomography*, vol. 17, pp. 201–204, September 2007.

[10] Y. V. Gulyaev, A. V. Korjenevsky, T. S. Tuykin, and V. A. Cherepenin, "Vizualizing electrically conducting media by electric field tomography," *Journal of Communications Technology and Electronics*, vol. 55, no. 9, pp. 1062–1069, 2010.

[11] M. Bertero, M. Miyakawa, P. Boccacci, F. Conte, K. Orikasa, and M. Furutani, "Image restoration in chirp-pulse microwave CT (CP-MCT)," *IEEE Transactions on Biomedical Engineering*, vol. 47, no. 5, pp. 690–699, 2000.

[12] J. D. Shea, P. Kosmas, B. D. van Veen, and S. C. Hagness, "Contrast-enhanced microwave imaging of breast tumors: a computational study using 3D realistic numerical phantoms," *Inverse Problems*, vol. 26, Article ID 074009, 2010.

[13] L. Lizzi, P. Rocca, A. Massa, T. Fujimoto, and T. Takenaka, "Synthesis of a wideband antenna array for microwave imaging applications," in *Proceedings of the 5th European Conference on Antennas and Propagation (EUCAP '11)*, pp. 1938–1941, April 2011.

[14] K. Suzuki and Y. Kuwahara, "Microwave mammography using multi-static UWB radar," in *Proceedings of the IEEE International Symposium on Antennas and Propagation and USNC/URSI National Radio Science Meeting (APSURSI '09)*, June 2009.

[15] I. Hieda and K. C. Nam, "FDTD simulation of radio imaging method for biomedical application," in *Proceedings of the 4th Kuala Lumpur International Conference on Biomedical Engineering (Biomed '08)*, pp. 566–569, Springer, Kuala Lumpur, Malaysia, June 2008.

[16] I. Hieda and K. C. Nam, "Improvement on signal strength detection of radio imaging method for biomedical application," in *Proceedings of the 13th International Conference on Biomedical Engineering (ICBME '08)*, vol. 23, pp. 523–526, Springer, Singapore, 2008.

[17] I. Hieda and K. C. Nam, "The frequency dependence of the effect of the human body conductivity in the radio imaging method for medical application," in *Proceedings of the 6th World Congress of Biomechanics (WCB '10)*, pp. 1562–1565, Singapore, August 2010.

[18] A. Taflove and S. C. Hagness, *Computational Electrodynamics*, The Finite-Difference Time-Domain Method, Artech House, London, UK, 2 edition, 2000.

[19] R. Lytle, "The numeric python EM project," *IEEE Antennas and Propagation Magazine*, vol. 44, no. 6, p. 146, 2002 (Japanese).

[20] M. Miyakawa, "Noninvasive measurement of temperature profiles inside dielectric materials," *Bulletin of the Electrotechnical Laboratory*, vol. 45, no. 9-10, pp. 419–435, 1981.

[21] E. Grayver, *Implementing Software Defined Radio*, Springer, New York, NY, USA, 2012.

[22] I. Hieda and K. C. Nam, "Electric field measurement for biomedical application using GNU radio," in *Proceedings of the 5th Kuala Lumpur International Conference on Biomedical Engineering (BIOMED '11)*, pp. 300–304, June 2011.

[23] "Ettus research," http://www.ettus.com/.

[24] "GNU radio," http://gnuradio.org/.

[25] I. Hieda and K. C. Nam, "Improvement of the measurement quality of radio imaging method for biomedical application," in *Proceedings of the World Congress on Medical Physics and Biomedical Engineering (WC '09)*, pp. 128–131, Springer, September 2009.

[26] I. Hieda, K. C. Nam, and A. Takahashi, "Basic characteristics of the radio imaging method for biomedical applications," *Medical Engineering and Physics*, vol. 26, no. 5, pp. 431–437, 2004.

[27] I. Hieda, "Preliminary study of 2D image construction by radio imaging method (RIM) for medical application," in *Proceedings of the Kuala Lumpur International Conference on Biomedical Engineering (IFMBE '04)*, vol. 7, pp. 91–94, Kuala Lumpur, Malaysia, September 2004.

[28] K. C. Nam and I. Hieda, "Dielectric measurement using radio imaging method for tomography," in *Proceedings of the 13th International Conference on Electrical Bioimpedance and the 8th Conference on Electrical Impedance Tomography (ICEBI '07)*, pp. 472–475, September 2007.

[29] T. Yahagi, "A deterministic approach to optimal linear digital equalizers," *IEEE Transactions on Acoustics, Speech, and Signal Processing*, vol. 31, no. 2, pp. 491–500, 1983.

[30] T. Yahagi, *Theory of Digital Signal Processing 2*, Corona Publishing, Tokyo, Japan, 1985.